NEUROLINGUISTICS

Distinct distributed patterns of neural activity are associated with two languages in the bilingual brain

Min Xu,[1,2] Daniel Baldauf,[3,4] Chun Qi Chang,[1,2] Robert Desimone,[3]* Li Hai Tan[1,2]*

A large body of previous neuroimaging studies suggests that multiple languages are processed and organized in a single neuroanatomical system in the bilingual brain, although differential activation may be seen in some studies because of different proficiency levels and/or age of acquisition of the two languages. However, one important possibility is that the two languages may involve interleaved but functionally independent neural populations within a given cortical region, and thus, distinct patterns of neural computations may be pivotal for the processing of the two languages. Using functional magnetic resonance imaging (fMRI) and multivariate pattern analyses, we tested this possibility in Chinese-English bilinguals when they performed an implicit reading task. We found a broad network of regions wherein the two languages evoked different patterns of activity, with only partially overlapping patterns of voxels in a given region. These regions, including the middle occipital cortices, fusiform gyri, and lateral temporal, temporoparietal, and prefrontal cortices, are associated with multiple aspects of language processing. The results suggest the functional independence of neural computations underlying the representations of different languages in bilinguals.

INTRODUCTION

The human brain has been equipped with a marked ability to acquire more than one language, as in bilingual individuals. However, it remains unsolved as to how different languages are represented in the bilingual brain (1–4). A large body of neuroimaging studies has suggested that multiple languages are processed and organized in a single brain system (5–7) [but see related studies (8–10)]. Brain areas are activated to a comparable degree when bilinguals performed tasks in the first (L1) and second (L2) languages at both the word level and the sentence level (11–19), although differential activation may be seen in some studies because of different proficiency levels and/or age of acquisition of the two languages (8, 15, 20, 21).

The traditional single cortical mechanism hypothesis assumes that shared regions are recruited for processing L1 and L2, but one important possibility is that the two languages may involve interleaved but functionally independent neural populations, and thus, distinct patterns of neural computations may be pivotal for the processing of the two languages. Bilingual speakers are able to use each of their languages appropriately and swiftly switch from one language to the other. It is therefore reasonable to hypothesize that there might be some degree of segregation in the neural representations of each language to avoid cross-talk (22, 23). In the typically used univariate analysis of functional neuroimaging data, images are spatially smoothed, and each voxel is treated independently, which leads to loss of fine-grained pattern information (24, 25). Multivariate pattern analysis (MVPA) extracts the signal that is present in the pattern of response across multiple voxels, and it could therefore resolve this problem by operating on patterns of neural activation and by directly linking activation patterns to experimental conditions (24, 26, 27). It is suited for detecting fine-grained pattern differences even if they occur in the absence of regional-average differences (28).

Here, we used MVPA and investigated whether the neural representations of L1 were distinguishable from those of L2 by analyzing the pattern of functional magnetic resonance imaging (fMRI) blood-oxygen-level dependent (BOLD) signals in Chinese-English bilinguals. We used an implicit word-processing task in which the subjects pressed a key when two consecutive words were the same (Fig. 1). The implicit reading task does not ask for explicit reading, but reading occurs obligatorily, and it provides comparable processing demands for different groups of subjects or conditions (29, 30). By using region of interest (ROI)–based and searchlight-based MVPA, we found a broad network of regions wherein the two languages evoked different patterns of activity.

RESULTS

Behavioral results

Reaction time and accuracy data were submitted to repeated-measures analysis of variance (ANOVA). The results showed that there was no significant effect for reaction time [$F(3, 33) = 0.61$, $P = 0.613$], but there was a significant effect for accuracy [$F(3,33) = 6.328$, $P < 0.01$]. Followed-up paired t tests revealed greater accuracy for Chinese real words than Chinese false fonts [$t(11) = 3.3$, $P < 0.01$] and English false fonts [$t(11) = 3.4$, $P < 0.01$] and greater accuracy for English real words than English false fonts [$t(11) = 2.9$, $P < 0.05$]. There were no significant differences in accuracy between Chinese real words and English real words [$t(11) = 1.33$, $P = 0.21$], between Chinese false fonts and English false fonts [$t(11) = 0.54$, $P = 0.60$], and between Chinese false fonts and English real words [$t(11) = 2.13$, $P = 0.06$] (as shown in Fig. 1B).

Multivoxel classification of L1 and L2

We first conducted MVPA to discriminate between L1 real words and L2 real words on the basis of ROIs that were consistently reported to be involved in reading and language processing according to previous studies (31–36), including the lateral occipital cortex (LOC; inferior/middle occipital cortex), fusiform gyrus (FusiG), lateral temporal cortex (LTC; superior/middle temporal gyri), temporoparietal cortex (TPC; supramarginal/angular gyri/inferior parietal lobule), and lateral prefrontal
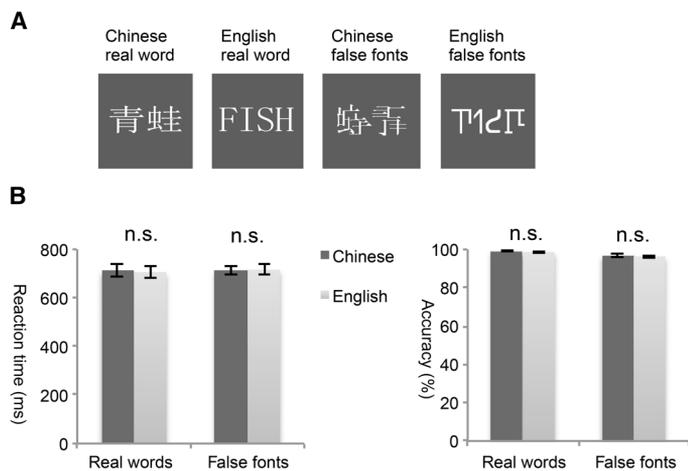
Fig. 1. Examples of experimental stimuli and behavioral performance. (**A**) Examples of Chinese real words, English real words, Chinese false fonts, and English false fonts used in the task. (**B**) Mean reaction time and accuracy rate for the four conditions. Error bars depict SEM. n.s., not significant.

Fig. 2. MVPA results for classification of L1 real words versus L2 real words. (**A**) Classification accuracies for the left (red bar) and right (blue bar) hemispheric ROIs. Error bars depict SEM. Significance markings for individual bars indicate above-chance (50%) classification accuracy; significance marking between bars indicates significant difference between left and right hemispheric ROIs. *$P <$ 0.05; **$P <$ 0.01; ***$P <$ 0.001. (**B**) Searchlight MVPA results presented as a T-map indicating the statistical significance of voxel-wise classification accuracies against the chance level [$P <$ 0.001, false discovery rate (FDR)–corrected, equivalent to $t =$ 5.2].

cortex (LPFC; inferior/middle frontal gyri) (fig. S1). Both the left and right hemispheric ROIs were defined. The results showed that the classification accuracies based on individual ROIs and the whole brain (WB) were all significantly greater than chance level (50%) after corrections for multiple comparisons (Fig. 2A): LOC [left: $t(13) =$ 29.3, $P <$ 0.0001; right: $t(13) =$ 19.4, $P <$ 0.0001]; FusiG [left: $t(13) =$ 21.6, $P <$ 0.0001; right: $t(13) =$ 13.4, $P <$ 0.0001]; LTC [left: $t(13) =$ 10.2, $P <$ 0.0001; right: $t(13) =$ 5.4, $P <$ 0.001]; TPC [left: $t(13) =$ 11.0, $P <$ 0.0001; right: $t(13) =$ 3.0, $P <$ 0.05]; LPFC [left: $t(13) =$ 9.7, $P <$ 0.0001; right, $t(13) =$ 4.5, $P <$ 0.001]; and WB [$t(13) =$ 13.4, $P <$ 0.0001]. We next performed a repeated-measures ANOVA with ROIs and the hemispheres as within-subject factors to explore hemispheric differences. Results revealed a significant main effect of hemisphere [$F(1,13) =$ 43.7, $P <$ 0.0001] and region [$F(4, 52) =$ 22.3, $P <$ 0.001]. There was a significant hemisphere × region interaction [$F(4, 52) =$ 3.7, $P <$ 0.05], indicating that the hemispheric effect was not the same across ROIs. To explore this, we performed post hoc paired t tests in each ROI separately and found that four ROIs showed significantly greater accuracies in the left than the right hemisphere: FusiG [$t(13) =$ 2.6, $P <$ 0.05]; LTC [$t(13) =$ 3.8, $P <$ 0.01]; TPC [$t(13) =$ 5.1, $P <$ 0.001]; and LPFC [$t(13) =$ 3.6, $P <$ 0.01], indicating that the left hemispheric ROIs carried more discriminative information than their right hemispheric counterparts. In contrast, there was no hemispheric difference in classification accuracy in LOC [$t(13) =$ 1.4, $P =$ 0.19]. To further examine whether classification of L1 versus L2 was mainly determined by positive BOLD response or negative BOLD response, we extracted the β values of the most informative voxels in the left hemispheric ROIs (see Materials and Methods). The analysis revealed that the classification accuracies were determined both by voxels with positive BOLD responses (36 to 74% of voxels across ROIs) and by voxels with negative BOLD responses (26 to 64% of voxels across ROIs) (fig. S2).

Searchlight MVPA
To ensure that we did not overlook any anatomical regions that were sensitive to L1 and L2, we used a "searchlight" approach to identify regions of high classification accuracy throughout the brain (37). As shown in Fig. 2B, analyses with a 4-mm-radius searchlight revealed left-lateralized discriminative patterns, with significant searchlight

centers located in the bilateral occipital cortex and fusiform gyri {peak at Montreal Neurological Institute (MNI) coordinates [−44 −64 −8] and [40 −70 −14]}, bilateral inferior and middle frontal gyri ([−46 12 28] and [54 28 8]), left TPC ([−58 −34 28]), and bilateral superior and middle temporal gyri ([−46 4 −4] and [58 −28 2]). This analysis also revealed sensitivity of the bilateral superior parietal lobule/precuneus (peak at [−24 −66 34] and [30 −74 38]) in distinguishing between L1 and L2. Therefore, in the following analyses, left and right superior parietal cortices (SPCs; superior parietal lobule/precuneus) were also included as ROIs.

Univariate analyses for L1 versus L2
Univariate analyses were conducted to facilitate comparisons between pattern-based and voxel-based analyses. We found several small clusters that showed greater activity for L2 real words than L1 real words in the left inferior frontal gyrus, left occipitotemporal cortex, and left precuneus (Fig. 3 and table S1), whereas no greater activity was found for L1 than L2, indicating that brain activation elicited by L1 and L2 overlapped substantially. Relative to univariate analyses, MVPA revealed markedly widespread brain regions that could successfully discriminate between L1 and L2 by incorporating the signal from multiple voxels.

Discriminative information in the ROIs
First, to examine whether the discriminative information concerns only low-level visual complexities that are distinct for the two languages, we applied the classifiers trained to distinguish between L1 and L2 real words to classify L1 and L2 false fonts (see Materials and Methods). Because the false fonts have similar structure and complexity to the real words but contain no linguistic features, the generation of activation

L2 > L1
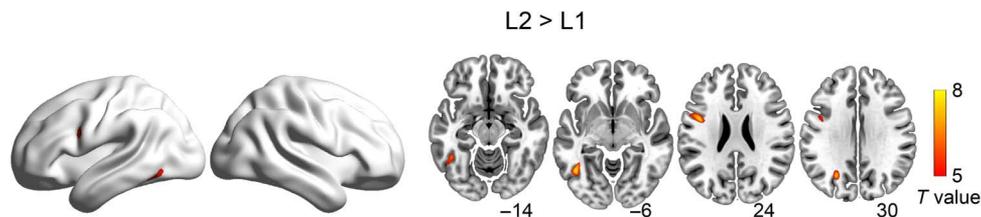
Fig. 3. Cortical activation associated with L2 real words minus L1 real words revealed by the univariate analysis ($P < 0.05$, FDR-corrected, equivalent to $t = 5.0$). No significant activation was found for L1 real words minus L2 real words.
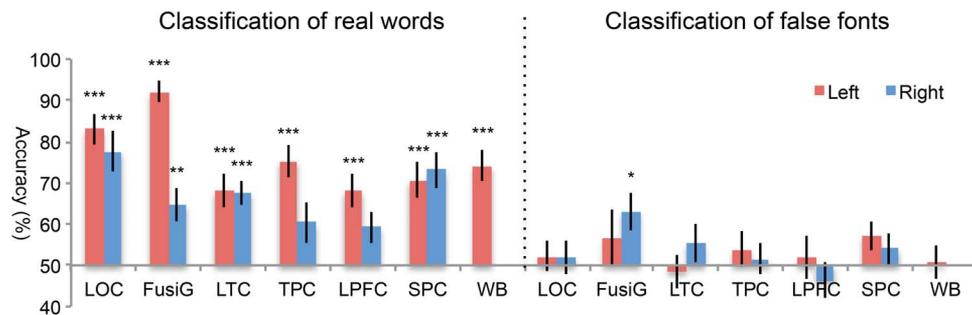
Fig. 4. Accuracies for classifying real words (left) and false fonts (right) between different languages using SVM classifier trained to discriminate between L1 and L2 real words. Error bars depict SEM. Significant above-chance (50%) classification accuracy is indicated by asterisks. *$P < 0.05$; **$P < 0.01$; ***$P < 0.001$.

patterns between real words and false fonts may indicate that L1 and L2 real words are distinguished on the basis of their visual complexity rather than differences in linguistic features of the two languages. As shown in Fig. 4, accuracies for classifying L1 and L2 real words were significantly greater than chance for most of the ROIs except in the right TPC and right LPFC. The accuracies in this step were lower than those obtained in the above ROI analyses, as shown in Fig. 2A, which may be due to less training data used (24). Accuracies for classifying L1 false fonts and L2 false fonts were statistically significant only in the right FusiG [$t(13) = 2.9$, $P < 0.05$] but not in any other ROI. We then performed a correlation analysis between the accuracies for classifying L1 and L2 real words and the accuracies for classifying L1 and L2 false fonts across ROIs. The result shows that the correlation is not significant ($r = 0.238$, $P = 0.434$) (fig. S3), suggesting that the regions containing the most discriminative information for L1 real words versus L2 real words do not necessarily contain the most discriminative information for L1 false fonts versus L2 false fonts. Correlation analyses were also performed within each ROI to examine whether the accuracies for classifying real words correlated with the accuracies for classifying false fonts of the two languages across subjects. We found significant correlation only in the right FusiG ($r = 0.576$, $P = 0.031$) but not in any other ROI. These results suggested that in most of the ROIs, activity patterns distinguishing between L1 real words and L2 real words were not based on low-level visual complexity.

Second, the frontal and parietal regions that we defined as language ROIs also belong to the domain-general frontoparietal executive network, which has been shown to decode different aspects of task demands and materials [see the study of Woolgar et al. (38) for a recent review]. To examine whether the voxels within these ROIs responded more strongly to words than false fonts, we performed a univariate analysis on (Chinese real words + English real words) versus (Chinese false fonts + English false fonts). The activation maps (threshold set at $P < 0.05$, FDR-corrected at voxel level) were masked by the anatomical ROIs of LPFC, TPC, and SPCs, respectively. We then

compared the number of voxels that activated for real words − false fonts (language-responsive) and the number of voxels that activated for false fonts − real words (cognitive demand–sensitive) [for a similar rationale, see the study of Fedorenko et al. (39)]. Results showed that there were much more language-responsive than cognitive demand–sensitive voxels in the LPFC (1940 versus 338) and TPC (1319 versus 599), suggesting that these two ROIs may distinguish between L1 and L2 more on the basis of the language-related information. In contrast, there were much fewer language-responsive voxels in the SPC (555 versus 1718), indicating that this region may rely more on the domain-general information to distinguish between the two languages.

Spatial distribution of the most informative voxels coding for L1 and L2

To examine the extent to which the most informative voxels coding for L1 were separated from those for L2, we performed classifiers in the left hemispheric ROIs for the two languages separately: L1 real words versus L1 false fonts (L1 discrimination) and L2 real words versus L2 false fonts (L2 discrimination). We found high classification accuracies for both L1 discrimination (90.6 to 97.6%) and L2 discrimination (84.4 to 96.6%) in all ROIs (fig. S4). We then generated maps for the best-coding voxels by including voxels whose weights exceeded 2 SD in the group analysis. The most informative voxels coding for L1 were spatially separated from those for L2 mainly in the left FusiG, LTC, TPC, LPFC, and SPC (Fig. 5, B to F), with separation percentages as follows: FusiG, 96.5%; LTC, 79.7%; TPC, 74.8%; LPFC, 67.3%; and SPC, 72.5% (the number of best-coding voxels surviving threshold is reported in table S2). In addition, we found considerable overlap of informative voxels between the two languages mainly in the left LOC (Fig. 5A; separation percentage, 50.1%). To facilitate a comparison between the univariate approach and MVPA, we followed a similar procedure to calculate the separation percentages for the univariate method in the left hemispheric ROIs. The separation percentages for individual ROIs yielded from the univariate analysis are as follows: LOC, 9.6%; FusiG,

L1 (red) **L2** (blue) **Overlap** (yellow)
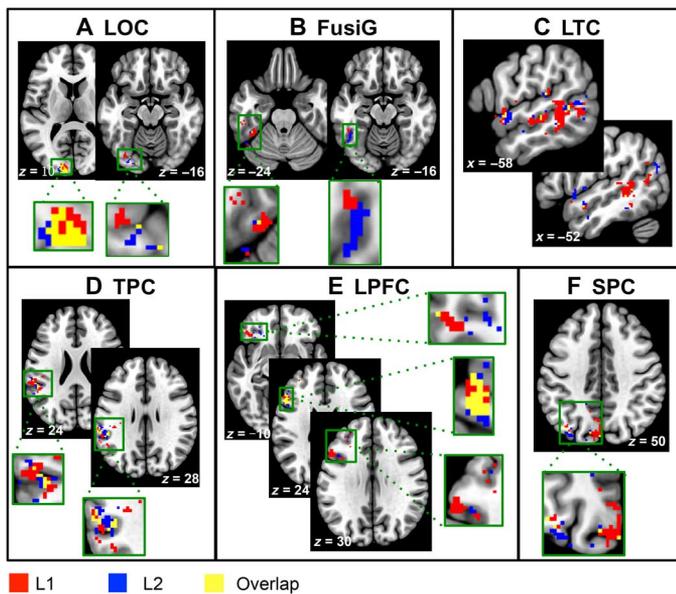
Fig. 5. Spatial distribution of the most informative voxels coding for L1 and L2. The maps show the best-coding voxels for L1 discrimination (red), L2 discrimination (blue), and their overlap (yellow) in the left hemispheric LOC (**A**), FusiG (**B**), LTC (**C**), TPC (**D**), LPFC (**E**), and SPC (**F**).

32.3%; LTC, 30.0%; TPC, 22.5%; LPFC, 28.5%; and SPC, 28.3% (fig. S5 and table S3), which are much less than those from MVPA.

DISCUSSION

Previous neuroimaging studies using the traditional univariate analyses have consistently found overlapping regions for L1 and L2 [for example, (11–19)]. Here, by using a more fine-grained MVPA technique, our study has demonstrated that different languages were processed in common regions but in distinguishable patterns of response, implicating that functionally independent neural populations are involved (28). Segregation in the neural representations of each language might be crucial for bilingual speakers to appropriately use each language and avoid cross-talk.

Previous aphasic and neurosurgical studies have supported distinct brain systems for different languages in bilinguals. Observations of brain-damaged patients showed that brain injuries may produce selective impairments of only one language in bilinguals and that patients may recover one language but not the other (40–45). Neurosurgical studies have also identified language-specific areas in dominant frontal, parietal, and temporal regions because electrical stimulation of these sites produces interferences in only one language and not in any other (46–50). Our findings may provide some implications for the evidence from neuroimaging and aphasic/neurosurgical studies. The MVPA that we used here discriminates neural representations of different languages by taking into account the relationships across voxels, whereas the univariate method previously used examines only changes in the gross neural activity and may therefore fail to detect the important differential patterns. Meanwhile, our results suggest that L1 and L2 are represented in specific patterns that involve neuronal populations in the critical regions to different degrees, such that electrical stimulation or inhibition of the neuron populations crucial for one language could cause interference of that language but not the other.

One question to address is what sort of information decoded by the brain distinguishes between L1 and L2. The implicit reading task that we used here is not designed to address any specific aspect of language processing, and thus, different brain regions that show distinct neural patterns may be associated with different levels of language processing. Written Chinese presents sharp contrast to English in terms of orthographic features and how the written symbols map onto sounds and semantics (51, 52). Therefore, information about the visual appearance, orthography, phonology, and semantics of the word stimuli could be used to classify the two languages. Chinese characters are formed with intricate strokes filled in square configurations, as opposed to the linear structure of alphabetic words. This difference may lead to the neural separations in the LOCs and the fusiform gyri for the representations of visual features and orthographic properties (30, 34, 36, 53) and in the SPCs for fine-grained visuospatial representations of written words in the two languages (54, 55). Moreover, Chinese characters map directly to monosyllables in an arbitrary way with tonal information that convey different meanings of words, whereas English is a nontonal language, and words are predominantly read out by assembling the phonemic components (32, 56). Distinct neural patterns in the temporal and lateral prefrontal cortices for the two languages may thus reflect their differences in phonological representations and in the mapping from written symbols to sound and meaning (31, 33, 35, 36). We also found that the distinct patterns for L1 and L2 in most regions are unlikely to reflect different visual complexities of the two languages because the support vector machine (SVM) classifier trained to discriminate between response patterns of Chinese real words and English real words failed to classify their corresponding false-font stimuli in all ROIs, except in the right FusiG, which may be recruited for holistic and configural analysis of the stimulus (57). Therefore, the differences in linguistic features might contribute to the discrimination between the two languages. Further research will need to more specifically examine the nature of the discriminative information, including comparing the auditory versus visual representations of words, to know whether the mapping between written forms and sound/meaning contributes to the classification.

Previous studies using MVPA to classify L1 and L2 have focused on specific sets of regions and produced inconsistent results (58–60). For example, Willms et al. (58) found no difference in multivoxel patterns for L1 and L2 in Spanish-English bilinguals, but they performed MVPA on ROIs restricted to these regions that showed greater activity for verb than noun processing in both L1 and L2. There was little overlap between the voxels in the ROIs and those in the regions that showed an interaction effect of language and grammatical class. Thus, the brain areas that were likely to distinguish between L1 and L2 were not included in the MVPA in the study. In another study, Bai et al. (60) found similar spatial patterns of response in visual word form areas to different languages in Korean-Chinese bilinguals, which is inconsistent with our results. One possibility is that written words of Korean and Chinese are both in square shape, and it might therefore be more difficult to discriminate them in the fusiform areas. An alternative (but not mutually exclusive) explanation is that Bai et al. (60) performed MVPA based on very restricted ROIs (6-mm radius centered at the peak of Chinese + Korean − fixation), whereas we used the whole FusiG as a priori anatomical ROIs. A recent study by Hsu et al. (59) investigated the emotional aspect of language processing and found distinguishable patterns for L1 and L2 in German-English bilinguals in emotion-related regions. Because these regions are not closely associated with language

processing, the study does not necessarily address the question of pattern differences between L1 and L2 per se.

Note that our findings do not imply that there are no shared representations for different languages in the bilingual brain. On the contrary, we identified a number of subsets of informative voxels overlapping for L1 and L2. This was consistent with previous MVPA findings that representations of semantic information can be generalized between L1 and L2 (61, 62) and with results from studies using fMRI adaptation paradigms that found language-independent semantic representations in the left lateral prefrontal (63, 64) and temporal regions (18, 63).

Together, we demonstrated here that L1 and L2 could be neuroanatomically separated by widely distributed patterns of activity using the pattern analysis technique. The finding may provide new leverage points for examining the underlying neural processes for different languages and thus offers an insight into the links between brain representations and language disorders in bilinguals. We note that the present study has limitations that should be addressed in the future. For example, although the subjects' behavioral performance on the task was comparable for L1 and L2, nonequivalent proficiency of L1 and L2 might have confounded the MVPA results. Further research is needed to more specifically examine the nature of these signals related to L1 and L2 in various brain areas, including whether they are modulated by proficiency and age of acquisition.

MATERIALS AND METHODS
Subjects
Fourteen bilingual subjects (12 females) were recruited in our experiment (aged 23 to 33 years; mean = 26.5, SD = 3.3). They were native Mandarin Chinese speakers from China and were studying or working in the Boston area during the time of scanning. The subjects had started to learn English as their L2 between 6 and 15 years of age. They completed a language-background questionnaire (65) and were measured of L2 proficiency using Peabody Picture Vocabulary Test (PPVT4) (mean score = 149.2, SD = 28.5). The subjects were physically healthy and free of neurological disease, head injury, and psychiatric disorder. They were right-handed, as assessed by the handedness inventory. The study was approved by the ethics committee at the Massachusetts Institute of Technology (MIT), and all subjects gave informed consent before the experiments.

Design and materials
The subjects performed an implicit word-processing task, in which they were presented with a sequence of words and required to press a key when two consecutive words were the same. The task was simple, providing comparable processing demands for L1 and L2. Animal words and action words were used for both languages. To match Chinese words and English words in length, we chose Chinese words containing two characters (average number of phonemes = 4.9, SD = 0.9; mean frequency = 11.5 per million) and English words containing three to six letters (average number of syllables = 1.1, SD = 0.3; average number of phonemes = 3.3, SD = 0.7; mean frequency = 26.5 per million). Chinese words were the closest possible translation of the English words, and thus, they were matched for meaning. The subjects also performed the task with false fonts, which were constructed by scrambling the strokes of the words used in the real-word conditions. With this method, the false fonts have a similar complexity to the real words but contain no linguistic features (Fig. 1A). The subjects underwent

six to eight functional runs. There were four blocks for each condition within each run, and condition order was counterbalanced. Each block consisted of 16 stimuli, among which 2 would be the same as the last one. On each trial, a white stimulus was displayed on the center of a gray background for 700 ms, followed by a 300-ms blank interval. To reduce practice effects, we used two different sets of stimulus items alternatively among different runs. All subjects had some practice before scanning, and they were instructed to perform as quickly and accurately as possible. We failed to record two subjects' behavioral responses, and thus, the behavioral results were based on data from the remaining 12 subjects. Their behavioral performance under each condition is illustrated in Fig. 1B.

MRI acquisition
Functional images were acquired using a 3T Siemens MRI scanner with a 32-channel head coil at the Athinoula A. Martinos Imaging Center at MIT. A gradient–echo echo planar imaging (EPI) sequence was used (TR (repetition time)/TE (echo time) = 2000/30 ms; flip angle = 90°; voxel size of 3.1 × 3.1 × 3, with a 0.3-mm gap). Visual stimuli were presented through a projector onto a translucent screen, and subjects viewed the screen through a mirror attached to the head coil.

fMRI data preprocessing and univariate analysis
We used the Statistical Parametric Mapping software package (SPM8) (www.fil.ion.ucl.ac.uk/spm/) for preprocessing. Functional images were realigned to the first volume of the first functional scan to remove movement artifact. They were then spatially normalized to an EPI template based on the International Consortium for Brain Mapping (ICBM) 152 stereotactic space. Voxels were resampled at a voxel size of $2 \times 2 \times 2$ mm^3. For the MVPA, functional images were not spatially smoothed. For the univariate analyses, an isotropic Gaussian kernel of 8 mm full width at half maximum (FWHM) was applied for spatial smoothing. The preprocessed images were passed to a general linear modeling (GLM), which was used to obtain parameter estimate (β) images associated with each stimulus condition. GLM was constructed with experimental regressors modeled as boxcar function and convolved with a canonical hemodynamic response function. Realignment parameters were included in the model to regress out movement-related variance. Each time series was high-pass–filtered with a cutoff period set at 128 s to remove low-frequency drifts. For the univariate analysis, contrast images were generated for each subject and were then used to create group contrast images at the second level.

Multivoxel pattern analyses
A linear support vector machine (LibSVM; regularization parameter C = 1) was performed using PRoNTo (for ROI approach) (66) and the Decoding Toolbox (for searchlight approach) (67). The β images were extracted for each run separately and used as input for the classifiers. We calculated the accuracy for classification using a leave-one-session-out cross-validation procedure. For MVPA based on ROIs, an SVM was trained and tested separately on WB and each ROI. Anatomical ROIs were generated using the Wake Forest University PickAtlas. For the statistical tests of classification accuracies across ROIs, results were corrected for multiple comparisons using FDR at $P = 0.05$ following the Benjamini-Hochberg procedure. To examine whether the classification accuracies of L1 and L2 were determined by positive BOLD response, negative BOLD response, or a combination of the two, we extracted the β values of the most

informative voxels. Linear SVM assigns a weight to each voxel that indicates its importance in the classification. The most informative voxels were defined as those voxels whose weights exceeded ±2 SD in the group analysis. We calculated the percentages of voxels with positive BOLD response (positive β value) and negative BOLD response (negative β value), as well as the averaged β values for each left hemispheric ROI.

In searchlight-based MVPA, a spherical searchlight with a radius of 4 mm was moved across the entire brain by taking each voxel in the volume as the searchlight center. For each sphere, a linear SVM was trained and tested as described above, and the classification accuracy score was assigned to the central voxel. The WB classification accuracy maps of individual subjects were spatially smoothed at 6-mm FWHM and were then subjected to random-effect group analysis. The resulted T-map indicated the statistical significance of voxel-wise accuracies against a chance-level accuracy of 50%. The T-map was thresholded at $P < 0.001$ and FDR-corrected.

To test whether the discriminative information concerns only low-level visual complexities that are distinct for L1 words and L2 words, we trained SVM classifiers to discriminate between response patterns of L1 real words and L2 real words and tested their predictive capacity for discriminating between L1 false fonts and L2 false fonts. We split the data set into two parts, with the first half as training data and the second half as testing data. The SVM classifiers were trained with the first half of real words, and the trained classifiers were then applied to predict the second half of real words and false fonts separately.

Finally, to examine spatial distributions of the most informative voxels coding for L1 and L2, we performed SVM classifiers using leave-one-session-out cross-validation for the two languages separately: L1 real words versus L1 false fonts (L1 discrimination) and L2 real words versus L2 false fonts (L2 discrimination). We generated maps for the left hemispheric ROIs to include the most informative voxels whose weights exceeded 2 SD in the group analysis. To quantify the different spatial distributions of informative voxels between L1 and L2, percentages of unique voxels were calculated for each language by dividing the number of unique voxels (that is, voxels for one language that do not show overlap with the other language) by the total number of voxels surviving threshold. Separation percentages were then calculated by averaging percentages of unique voxels for L1 and L2, that is, $(L1_{unique}/L1 + L2_{unique}/L2)/2$. To compare the degrees of spatial separation of L1 versus L2 using different approaches, we followed a similar procedure as in the MVPA to calculate the separation percentages in the univariate analysis. Contrast images of L1 real words minus L1 false fonts and L2 real words minus L2 false fonts were generated for each subject, and at the second-level analysis, anatomical ROIs were used as masks to create group contrast images. The most activated voxels with activation levels exceeding 2 SD in the group analysis were used to calculate separation percentages.

SUPPLEMENTARY MATERIALS

Supplementary material for this article is available at http://advances.sciencemag.org/cgi/content/full/3/7/e1603309/DC1

fig. S1. Axial view of ROIs overlaid on standard brain.
fig. S2. Percentages and the averaged β values of the voxels showing positive (red) and negative (blue) BOLD responses among the voxels contributing the most to the classification of L1 real words versus L2 real words in each of the left hemispheric ROIs.
fig. S3. Correlation between the accuracies for classifying L1 and L2 real words and the accuracies for classifying L1 and L2 false fonts across ROIs.
fig. S4. Accuracies for classifying L1 real words versus L1 false fonts (L1 discrimination, left panel) and classifying L2 real words and L2 false fonts (L2 discrimination, right panel).

fig. S5. Spatial distribution of the activated voxels for L1 and L2 in the univariate analysis.
table S1. Coordinates of activation peaks for the contrast of English words minus Chinese words in the univariate analysis.
table S2. Number of best-coding voxels surviving threshold ($z > 2$) and percentages of unique voxels for L1 and L2 for each ROI in MVPA.
table S3. Number of voxels surviving the threshold ($z > 2$) and percentages of unique voxels for L1 and L2 for each ROI in the univariate analysis.

REFERENCES AND NOTES

1. T. M. H. Hope, Ō. Parker Jones, A. Grogan, J. Crinion, J. Rae, L. Ruffle, A. P. Leff, M. L. Seghier, C. J. Price, D. W. Green, Comparing language outcomes in monolingual and bilingual stroke patients. *Brain* **138**, 1070–1083 (2015).
2. P. Li, Lexical organization and competition in first and second languages: Computational and neural mechanisms. *Cogn. Sci.* **33**, 629–664 (2009).
3. A. E. Hernandez, *The Bilingual Brain* (Oxford Univ. Press, 2013).
4. M. T. Ullman, A cognitive neuroscience perspective on second language acquisition: The declarative/procedural model, in *Mind and Context in Adult Second Language Acquisition*, C. Sanz, Ed. (Georgetown Univ. Press, 2005), pp. 141–178.
5. D. W. Green, Bilingual aphasia: Adapted language networks and their control. *Annu. Rev. Appl. Linguist.* **28**, 25–48 (2008).
6. J. Abutalebi, S. F. Cappa, D. Perani, The bilingual brain as revealed by functional neuroimaging. *Biling. Lang. Congn.* **4**, 179–190 (2001).
7. D. Perani, J. Abutalebi, The neural basis of first and second language processing. *Curr. Opin. Neurobiol.* **15**, 202–206 (2005).
8. K. H. S. Kim, N. R. Relkin, K.-M. Lee, J. Hirsch, Distinct cortical areas associated with native and second languages. *Nature* **388**, 171–174 (1997).
9. W. W. P. Tham, S. J. R. Liow, J. C. Rajapakse, T. C. Leong, S. E. S. Ng, W. E. H. Lim, L. G. Ho, Phonological processing in Chinese–English bilingual biscriptals: An fMRI study. *Neuroimage* **28**, 579–587 (2005).
10. L. H. Tan, L. Chen, V. Yip, A. H. D. Chan, J. Yang, J.-H. Gao, W. T. Siok, Activity levels in the left hemisphere caudate–fusiform circuit predict how well a second language will be learned. *Proc. Natl. Acad. Sci. U.S.A.* **108**, 2540–2544 (2011).
11. D. Klein, B. Milner, R. J. Zatorre, E. Meyer, A. C. Evans, The neural substrates underlying word generation: A bilingual functional-imaging study. *Proc. Natl. Acad. Sci. U.S.A.* **92**, 2899–2903 (1995).
12. M. W. L. Chee, D. Caplan, C. S. Soon, N. Sriram, E. W. L. Tan, T. Thiel, B. Weekes, Processing of visually presented sentences in Mandarin and English studied with fMRI. *Neuron* **23**, 127–137 (1999).
13. L. H. Tan, J. A. Spinks, C.-M. Feng, W. T. Siok, C. A. Perfetti, J. Xiong, P. T. Fox, J.-H. Gao, Neural systems of second language reading are shaped by native language. *Hum. Brain Mapp.* **18**, 158–166 (2003).
14. F. Cao, R. Tao, L. Liu, C. A. Perfetti, J. R. Booth, High proficiency in a second language is characterized by greater involvement of the first language network: Evidence from Chinese learners of English. *J. Cogn. Neurosci.* **25**, 1649–1663 (2013).
15. D. Perani, E. Paulesu, N. S. Galles, E. Dupoux, S. Dehaene, V. Bettinardi, S. F. Cappa, F. Fazio, J. Mehler, The bilingual brain. Proficiency and age of acquisition of the second language. *Brain* **121**, 1841–1852 (1998).
16. J. Illes, W. S. Francis, J. E. Desmond, J. D. E. Gabrieli, G. H. Glover, R. Poldrack, C. J. Lee, A. D. Wagner, Convergent cortical representation of semantic processing in bilinguals. *Brain Lang.* **70**, 347–363 (1999).
17. S. Cherodath, N. C. Singh, The influence of orthographic depth on reading networks in simultaneous biliterate children. *Brain Lang.* **143**, 42–51 (2015).
18. J. Crinion, R. Turner, A. Grogan, T. Hanakawa, U. Noppeney, J. T. Devlin, T. Aso, S. Urayama, H. Fukuyama, K. Stockton, Language control in the bilingual brain. *Science* **312**, 1537–1540 (2006).
19. H. Liu, Z. Hu, T. Guo, D. Peng, Speaking words in two languages with one brain: Neural overlap and dissociation. *Brain Res.* **1316**, 75–82 (2010).
20. I. Wartenburger, H. R. Heekeren, J. Abutalebi, S. F. Cappa, A. Villringer, D. Perani, Early setting of grammatical processing in the bilingual brain. *Neuron* **37**, 159–170 (2003).
21. J. A. Berken, V. L. Gracco, J.-K. Chen, K. E. Watkins, S. Baum, M. Callahan, D. Klein, Neural activation in speech production and reading aloud in native and non-native languages. *Neuroimage* **112**, 208–217 (2015).
22. S. Dehaene, Fitting two languages into one brain. *Brain* **122**, 2207–2208 (1999).
23. M. Paradis, *A Neurolinguistic Theory of Bilingualism* (John Benjamins Publishing, 2004).
24. J.-D. Haynes, A primer on pattern-based approaches to fMRI: Principles, pitfalls, and perspectives. *Neuron* **87**, 257–270 (2015).
25. J. V. Haxby, Multivariate pattern analysis of fMRI: The early beginnings. *Neuroimage* **62**, 852–855 (2012).
26. K. A. Norman, S. M. Polyn, G. J. Detre, J. V. Haxby, Beyond mind-reading: Multi-voxel pattern analysis of fMRI data. *Trends Cogn. Sci.* **10**, 424–430 (2006).

27. A. J. O'Toole, F. Jiang, H. Abdi, N. Pénard, J. P. Dunlop, M. A. Parent, Theoretical, statistical, and practical perspectives on pattern-based classification approaches to the analysis of functional neuroimaging data. *J. Cogn. Neurosci.* **19**, 1735–1752 (2007).

28. M. Mur, P. A. Bandettini, N. Kriegeskorte, Revealing representational content with pattern-information fMRI—An introductory guide. *Soc. Cogn. Affect. Neurosci.* **4**, 101–109 (2009).

29. P. E. Turkeltaub, L. Gareau, D. L. Flowers, T. A. Zeffiro, G. F. Eden, Development of neural mechanisms for reading. *Nat. Neurosci.* **6**, 767–773 (2003).

30. E. Paulesu, E. McCrory, F. Fazio, L. Menoncello, N. Brunswick, S. F. Cappa, M. Cotelli, G. Cossu, F. Corte, M. Lorusso, S. Pesenti, A. Gallagher, D. Perani, C. Price, C. D. Frith, U. Frith, A cultural effect on brain function. *Nat. Neurosci.* **3**, 91–96 (2000).

31. C. J. Price, A review and synthesis of the first 20years of PET and fMRI studies of heard speech, spoken language and reading. *Neuroimage* **62**, 816–847 (2012).

32. L. H. Tan, A. R. Laird, K. Li, P. T. Fox, Neuroanatomical correlates of phonological processing of Chinese characters and alphabetic words: A meta analysis. *Hum. Brain Mapp.* **25**, 83–91 (2005).

33. J. D. E. Gabrieli, R. A. Poldrack, J. E. Desmond, The role of left prefrontal cortex in language and memory. *Proc. Natl. Acad. Sci. U.S.A.* **95**, 906–913 (1998).

34. S. Dehaene, L. Cohen, The unique role of the visual word form area in reading. *Trends Cogn. Sci.* **15**, 254–262 (2011).

35. S. Bookheimer, Functional MRI of language: New approaches to understanding the cortical organization of semantic processing. *Annu. Rev. Neurosci.* **25**, 151–188 (2002).

36. S. E. Shaywitz, R. Morris, B. A. Shaywitz, The education of dyslexic children from childhood to young adulthood. *Annu. Rev. Psychol.* **59**, 451–475 (2008).

37. N. Kriegeskorte, R. Goebel, P. Bandettini, Information-based functional brain mapping. *Proc. Natl. Acad. Sci. U.S.A.* **103**, 3863–3868 (2006).

38. A. Woolgar, J. Jackson, J. Duncan, Coding of visual, auditory, rule, and response information in the brain: 10 years of multivoxel pattern analysis. *J. Cogn. Neurosci.* **28**, 1433–1454 (2016).

39. E. Fedorenko, J. Duncan, N. Kanwisher, Language-selective and domain-general regions lie side by side within Broca's area. *Curr. Biol.* **22**, 2059–2062 (2012).

40. M. Paradis, Language and communication disorders in multilinguals, in *Handbook of the Neuroscience of Language*, B. Stemmer, H. Whitaker, Eds. (Elsevier Science/Academic Press, 2008), vol. 2, pp. 341–349.

41. F. Fabbro, The bilingual brain: Cerebral representation of languages. *Brain Lang.* **79**, 211–222 (2001).

42. E. Gomeztortosa, E. M. Martin, M. Gaviria, F. Charbel, J. I. Ausman, Selective deficit of one language in a bilingual patient following surgery in the left perisylvian area. *Brain Lang.* **48**, 320–325 (1995).

43. Y. Aladdin, T. J. Snyder, S. N. Ahmed, Pearls & Oysters: Selective postictal aphasia: Cerebral language organization in bilingual patients. *Neurology* **71**, e14–e17 (2008).

44. A. García-Caballero, I. García-Lado, J. González-Hermida, R. Area, M. J. Recimil, O. Juncos Rabadán, S. Lamas, G. Ozaita, F. J. Jorge, Paradoxical recovery in a bilingual patient with aphasia after right capsuloputaminal infarction. *J. Neurol. Neurosurg. Psychiatry* **78**, 89–91 (2007).

45. M. Meinzer, J. Obleser, T. Flaisch, C. Eulitz, B. Rockstroh, Recovery from aphasia as a function of language therapy in an early bilingual patient demonstrated by fMRI. *Neuropsychologia* **45**, 1247–1256 (2007).

46. G. A. Ojemann, H. A. Whitaker, The bilingual brain. *Arch. Neurol.* **35**, 409–412 (1978).

47. C. Giussani, F.-E. Roux, V. Lubrano, S. M. Gaini, L. Bello, Review of language organisation in bilingual patients: What can we learn from direct brain mapping? *Acta Neurochir.* **149**, 1109–1116 (2007).

48. T. H. Lucas II, G. M. McKhann II, G. A. Ojemann, Functional separation of languages in the bilingual brain: A comparison of electrical stimulation language mapping in 25 bilingual patients and 117 monolingual control patients. *J. Neurosurg.* **101**, 449–457 (2004).

49. F.-E. Roux, V. Lubrano, V. Lauwers-Cances, M. Trémoulet, C. R. Mascott, J.-F. Démonet, Intra-operative mapping of cortical areas involved in reading in mono- and bilingual patients. *Brain* **127**, 1796–1810 (2004).

50. J. A. Walker, A. Quiñones-Hinojosa, M. S. Berger, Intraoperative speech mapping in 17 bilingual patients undergoing resection of a mass lesion. *Neurosurgery* **54**, 113–118 (2004).

51. C. A. Perfetti, F. Cao, J. Booth, Specialization and universals in the development of reading skill: How Chinese research informs a universal science of reading. *Sci. Stud. Read.* **17**, 5–21 (2013).

52. W. T. Siok, C. A. Perfetti, Z. Jin, L. H. Tan, Biological abnormality of impaired reading is constrained by culture. *Nature* **431**, 71–76 (2004).

53. B. L. Schlaggar, B. D. McCandliss, Development of neural systems for reading. *Annu. Rev. Neurosci.* **30**, 475–503 (2007).

54. F. Cao, M. Vu, D. H. L. Chan, J. M. Lawrence, L. N. Harris, Q. Guan, Y. Xu, C. A. Perfetti, Writing affects the brain network of reading in Chinese: A functional magnetic resonance imaging study. *Hum. Brain Mapp.* **34**, 1670–1684 (2013).

55. M. Xu, T. Wang, S. Chen, P. T. Fox, L. H. Tan, Effective connectivity of brain regions related to visual word recognition: An fMRI study of Chinese reading. *Hum. Brain Mapp.* **36**, 2580–2591 (2015).

56. V. P. Y. Kwok, T. Wang, S. Chen, K. Yakpo, L. Zhu, P. T. Fox, L. H. Tan, Neural signatures of lexical tone reading. *Hum. Brain Mapp.* **36**, 304–312 (2015).

57. J. Dien, A tale of two recognition systems: Implications of the fusiform face area and the visual word form area for lateralized object recognition models. *Neuropsychologia* **47**, 1–16 (2009).

58. J. L. Willms, K. A. Shapiro, M. V. Peelen, P. E. Pajtas, A. Costa, L. R. Moo, A. Caramazza, Language-invariant verb processing regions in Spanish–English bilinguals. *Neuroimage* **57**, 251–261 (2011).

59. C.-T. Hsu, A. M. Jacobs, M. Conrad, Can Harry Potter still put a spell on us in a second language? An fMRI study on reading emotion-laden literature in late bilinguals. *Cortex* **63**, 282–295 (2015).

60. J. Bai, J. Shi, Y. Jiang, S. He, X. Weng, Chinese and Korean characters engage the same visual word form area in proficient early Chinese-Korean bilinguals. *PLOS ONE* **6**, e22765 (2011).

61. A. Buchweitz, S. V. Shinkareva, R. A. Mason, T. M. Mitchell, M. A. Just, Identifying bilingual semantic neural representations across languages. *Brain Lang.* **120**, 282–289 (2012).

62. J. Correia, E. Formisano, G. Valente, L. Hausfeld, B. Jansma, M. Bonte, Brain-based translation: fMRI decoding of spoken words in bilinguals reveals language-independent semantic representations in anterior temporal lobe. *J. Neurosci.* **34**, 332–338 (2014).

63. M. W. L. Chee, C. S. Soon, H. L. Lee, Common and segregated neuronal networks for different languages revealed using functional magnetic resonance adaptation. *J. Cogn. Neurosci.* **15**, 85–97 (2003).

64. D. Klein, R. J. Zatorre, J.-K. Chen, B. Milner, J. Crane, P. Belin, M. Bouffard, Bilingual brain organization: A functional magnetic resonance adaptation study. *Neuroimage* **31**, 366–375 (2006).

65. P. Li, S. Sepanski, X. Zhao, Language history questionnaire: A web-based interface for bilingual research. *Behav. Res. Methods* **38**, 202–210 (2006).

66. J. Schrouff, M. J. Rosa, J. M. Rondina, A. F. Marquand, C. Chu, J. Ashburner, C. Phillips, J. Richiardi, J. Mourão-Miranda, PRoNTo: Pattern recognition for neuroimaging toolbox. *Neuroinformatics* **11**, 319–337 (2013).

67. M. N. Hebart, K. Görgen, J.-D. Haynes, The Decoding Toolbox (TDT): A versatile software package for multivariate analyses of functional imaging data. *Front. Neuroinform.* **8**, 88 (2015).

Citation: M. Xu, D. Baldauf, C. Q. Chang, R. Desimone, L. H. Tan, Distinct distributed patterns of neural activity are associated with two languages in the bilingual brain. *Sci. Adv.* **3**, e1603309 (2017).

ScienceAdvances

Distinct distributed patterns of neural activity are associated with two languages in the bilingual brain

Min Xu, Daniel Baldauf, Chun Qi Chang, Robert Desimone and Li Hai Tan

ARTICLE TOOLS	http://advances.sciencemag.org/content/3/7/e1603309
SUPPLEMENTARY MATERIALS	http://advances.sciencemag.org/content/suppl/2017/07/10/3.7.e1603309.DC1
REFERENCES	This article cites 63 articles, 12 of which you can access for free http://advances.sciencemag.org/content/3/7/e1603309#BIBL
PERMISSIONS	http://www.sciencemag.org/help/reprints-and-permissions

Use of this article is subject to the Terms of Service